Adaptive Precision Training: Quantify Back Propagation in Neural Networks with Fixed-point Numbers

Xishan Zhang[1], **Shaoli Liu**[2], **Rui Zhang**[1], **Chang Liu**[1,3], **Di Huang**[1,3]
Shiyi Zhou[1,3], **Jiaming Guo**[1,3], **Yu Kang**[2], **Qi Guo**[1,3], **Zidong Du**[1], **Yunji Chen**[1,3]
{zhangxishan,zhangrui,liuchang18s,huangdi18s}@ict.ac.cn, liushaoli@cambricon.com
[1]Institute of Computing Technology, CAS, Beijing, China
[2]Cambricon Tech.Ltd, Beijing, China
[3]University of Chinese Academy of Sciences, Beijing, China

Abstract

Recent emerged quantization technique (i.e., using low bit-width fixed-point data instead of high bit-width floating-point data) has been applied to inference of deep neural networks for fast and efficient execution. However, directly applying quantization in training can cause significant accuracy loss, thus remaining an open challenge. In this paper, we propose a novel training approach, which applies a layer-wise precision-adaptive quantization in deep neural networks. The new training approach leverages our key insight that the degradation of training accuracy is attributed to the dramatic change of data distribution. Therefore, by keeping the data distribution stable through a layer-wise precision-adaptive quantization, we are able to directly train deep neural networks using low bit-width fixed-point data and achieve guaranteed accuracy, without changing hyper parameters. Experimental results on a wide variety of network architectures (e.g., convolution and recurrent networks) and applications (e.g., image classification, object detection, segmentation and machine translation) show that the proposed approach can train these neural networks with negligible accuracy losses (-1.40%∼1.3%, 0.02% on average), and speed up training by 252% on a state-of-the-art Intel CPU.

1. Introduction

While deep neural networks have become state-of-the-art techniques for a wide range of machine learning applications, such as image recognition [14], object detection [21], machine translation [32, 8], the computation costs of deep neural networks are continuously increasing, which greatly hampers the development and deployment of deep neural networks. For example, 10,000 GPU hours are used to perform neural architecture search on ImageNet [2]. Quantization is a promising technique to reduce the computation cost of neural network training, which can replace high-cost floating-point numbers (e.g., float32) with low-cost fixed-point numbers (e.g., int8/int16). Recently, both the software society [6, 12, 16, 19, 27, 35] and the hardware society [11, 24, 23, 31] have carried out extensive researches about quantization of deep neural network for inference tasks.

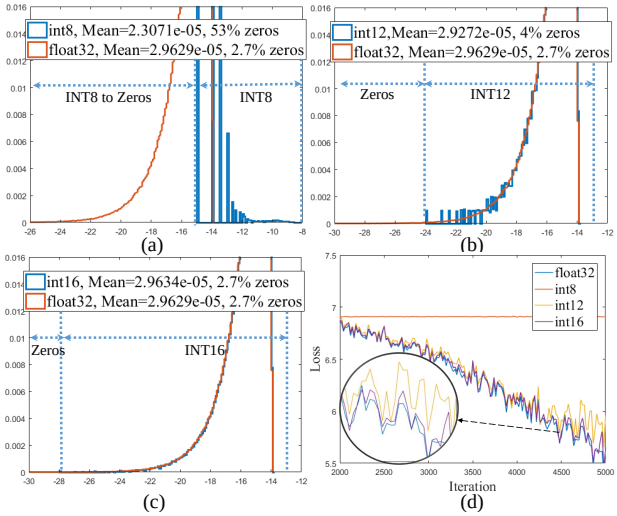

Figure 1: AlexNet fc2 layer activation gradient distribution (base-2 logarithm) and training convergence.

Though various investigations have demonstrated that deep learning inference can be accurately performed with low bit-width fixed-point numbers through quantization, the quantified training remains an open challenge. Some ex-

isting approaches quantify the backward-pass to low-bit (e.g., int8) but incur significant accuracy drop, for examples, 3˜7% loss for AlexNet [38, 36]. [7] uses int16 for both forward-pass and backward-pass to ensure accuracy. However, there is no guarantee that unified int16 precision works for all the tasks and networks.

Most previous investigations on quantified training use unified precision (i.e., bit-width) for all network layers. Intuitively, using mixed precisions for different layers will promote the network performance. However, it is hard to find the most appropriate precisions for so many layers in so many training iterations. Considering a widely used ResNet50 model, with 4 candidate quantization bit-widths (e.g., 8, 16, 24, 32 for weights, activations and activation gradients), the size of quantization precision combination search space for 450,000 training iterations can achieve $4^{3*50*450,000}$.

To avoid prohibitively long space searching of quantization bit-width combinations, we propose an efficient and adaptive technique to determine the bit-width layer by layer separately, which is based on our observation about the relationship between the layer-wise bit-width and the training convergence. Take AlexNet as an example, Figure. 1(a-c) depict the distributions of activation gradients on AlexNet last layer when quantified with different bit-widths. Compared with the original float32, int8 introduces a significant change in data distribution, int12 introduces slightly change of data mean, and int16 shows almost the same distribution with float32. Figure. 1(d) depicts the corresponding training loss, which shows int8 quantization does not converge at beginning, int12 convergences slower than float32 and int16 behaves similar as float32. The above experimental results suggest if a quantization resolution does not change the data distribution of a layer (e.g., int16 for the last layer of AlexNet), quantified training with this resolution for the corresponding layer will almost keep the training accuracy.

Based on the above observation, one can train large-scale deep neural network using fixed-point numbers, with no change of hyper parameters and no accuracy degradation. For each layer in training, our approach automatically finds the best quantization resolution (i.e., the smallest bit-width which does not significantly change the data mean) for weights, activations and activation gradients respectively. Concretely, we first calculate the mean of the data before quantization. Then, we quantify the data using int8 and calculate the quantization error. If the ratio of quantization error exceeds a threshold (e.g., 3%), the quantization bit-width is increased by 8. The above process is looped until the quantization error ratio is below the threshold.

We evaluate our approach on a wide variety of network architectures (e.g. convolution and recurrent networks) and applications (e.g. image classification, object detection, segmentation and machine translation). Our approach quantifies all weights and activations to int8. On average, 12.56%, 87.43% and 0.07% of activation gradients are quantified to int8, int16, and int24 respectively. Experimental results show that the proposed adaptive precision training approach can achieve comparable accuracy with float32 for training from scratch. The accuracy loss is only 0.02% on average (-1.40%$\sim$1.3%). Results on Intel Xeon Gold 6154 shows that the proposed approach can achieve 2.52 times speedup over float32 training for AlexNet.

We highlight three major contributions of the proposed adaptive precision training:

1. **Flexibility:** The quantization precisions for different layers of different networks are automatically adapted to guarantee the network accuracy.

2. **Efficiency:** We quantify both the backward-pass and forward-pass with fixed-point numbers in training, which can accelerate training on real hardware. After training, int8 weights can be directly deployed, so no further quantification is needed.

3. **Generalization:** Evaluations on various networks and applications demonstrate the proposed adaptive precision fixed-point training is effective and practical.

2. Related Works

Using reduced precision for deep learning has been an active research topic. Prior efforts explore floating-points(e.g., 8-bit and 16-bit) for training [34, 22] and maintain accuracy on a spectrum of deep learning models and datasets. However, as floating-point is more resource-intensive than fixed-point, the deployments always rely on quantization techniques.

A branch of work explores the fixed-point for forward prorogation(FPROP) [16, 17, 6, 33, 35, 35, 37]. The weights and activations are quantified to 1-8 bits. However, the backward-pass, including gradient propagation (BPROP), and weight gradient computation (WTGRAD) still require float32.

There are recent attempts quantifying weight and activation on different layers with different bit-widths. For the inference of a trained network, there are some techniques that heuristically search the space of quantization bit-width combinations [35, 33, 37]. However, these inference techniques only need to consider single iteration, whose search space is much smaller than training. Hence, they are unsuitable for training. For training, some differentiable quantization methods [4, 30, 37] learn the quantization parameters (e.g., step size, dynamic range and bit-width) with gradient descent. However, the quantization parameters for backward propagation are hard to learn using differentiable

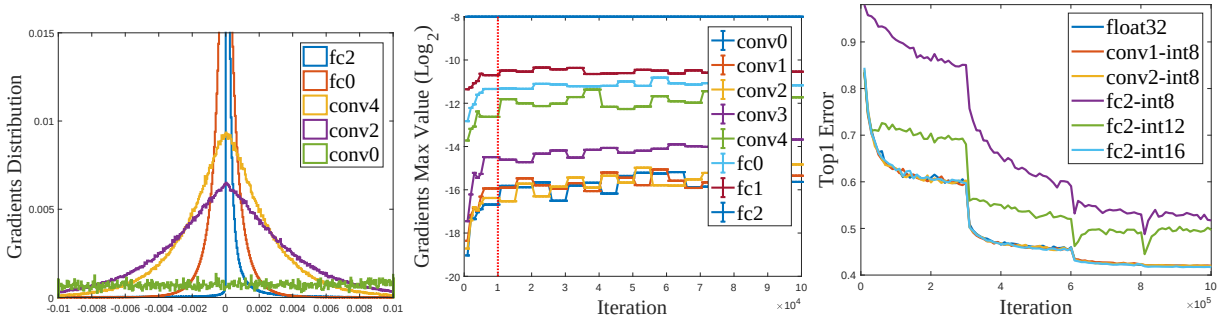

(a) Activation gradient distribution. (b) Activation gradient evolution. (c) Training curve of AlexNet.

Figure 2: Observations on AlexNet.

methods. [26] quantifies the backward propagation. Different from their method, which assigns layer-wise bit-width before training, our approach dynamically changes the bit-width during training and we evaluate on widely used networks.

Researchers have shown that 16-bit is sufficient for back propagation in most vision training tasks [7]. However, further quantization to 8-bit results in severe degradation [38, 38, 36, 7, 1]. WAGE [36] claims that first and last layers require higher precision. TBP [1] shows weight gradient computation (WTGRAD) needs more bits than gradient back propagation (BPROP).

Our approach is different from others in three aspects. First, fixed-point is used in both forward-pass and backward-pass for training. Second, the quantization parameters for different layers are dynamically adapted to guarantee the accuracy. Lastly, we train a variety of vision and natural language processing applications on large scale dataset.

3. Observation

The key of fixed-point training is to find proper quantization parameters that ensure the training accuracy. Therefore, we study the relationship between the ever-changing data distribution of different layers and the training convergence.

Observation 1. Data distribution varies greatly between layers. Figure. 2a depicts the distributions of activation gradients of different layers on AlexNet. The majority of activation gradients concentrate in areas close to zero, and have long tail distributions. Compared to convolution layers, the fully connected layers have larger variances. Figure. 2b shows the base-2 logarithm of max absolute value of activation gradients on AlexNet, the max value on bottom layers (e.g., conv0, conv1, conv2) is smaller than the max value on upper layers(e.g., fc0, fc1, fc2). Intuitively, for those layers whose range of data is wide and distribution is centralized, higher quantization resolutions are demanded.

Observation 2. Data range of each layer changes during training. Figure. 2b shows the max absolute value of activation gradient evolution during training. At the early stage of training (less than 10,000 iterations, as shown on the left side of the red line), the data range changes rapidly, and after one or two epochs, the data range tends to be stable. This phenomenon suggests that when training from scratch, the quantization range should also be changed frequently within the initial epochs .

Observation 3. Data with large variance requires large bit-width. Figure. 2c shows the convergence curves using different bit-width of different layers. Float32 is the training convergence curve of using float32 for all the convolution and fully connected layers. After 5,000,000 iterations, the network's top1 accuracy on ImageNet is 58.00%. Then, we quantify the activation gradients of conv1 to int8 and keep other layers float32. The training curve of conv1-int8 is the same as float32 and the final top1 accuracy is 58.01%. However, when we quantify the activation gradients of fc2 to int8 and keep other layers float32 unchanged, the training convergence speed is significantly slower than float32, and within the first 5,000 iterations the training does not converge. The final top1 accuracy of fc2-int8 is only 48.27%. When quantifying the activation gradients of fc2 to int12, the training convergence speed is faster than int8 but still slower than float32. The final top1 accuracy of fc2-int12 is only 50.30%. Using int16 for the activation gradients of fc2, finally the training curve is the same as float32 with 58.28% top1 accuracy. In conclusion, int8 is enough to quantify the activation gradient of conv2, however, fc2 requires int16 to maintain the training accuracy. Together with the observation1, we find that data with large variance requires large bit-width, thus the quantization parameters should be dynamically determined by the data distribution.

According to network initialization principle [10, 13], all network parameters are initialized as Gaussian distribution with variance relating to the hyper-parameters of layers. Similar network initialization principle and similar learning

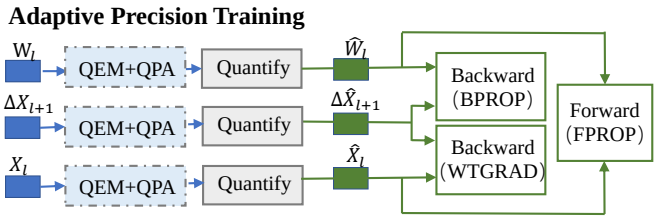

Figure 3: Adaptive precision training for one iteration one layer. The green nodes and blocks indicate fixed-point data and calculations. Only 0.01%∼2% of the iterations activate the QEM and QPA components.

algorithm ensure that our observations should be applicable on various network architectures.

4. Adaptive Precision Training

In this section, we introduce the adaptive precision training approach as shown in Figure. 3. In training, the main three computing units of single iteration include forward-pass (FPROP), backward-pass for gradient propagation (BPROP) and backward-pass for weight gradient computation (WTGRAD). The inputs of these three units include weight W_l, activation X_l and top layers' activation gradient ΔX_{l+1} of linear layer l. In adaptive precision training, we quantify these three inputs to fixed-point numbers[1]. The quantification parameters, such as bit-width n and quantization resolution r are automatically determined by the proposed Quantization Error Measurement (QEM) and Quantification Parameter Adjustment (QPA) .

In the following part of this section, we will introduce two main components QEM and QPA of our training approach. Algorithm. 1 describes the entire adaptive precision training algorithm. The output of QEM (denoted as $Diff$) serves as an explicit indicator for insufficiency of quantization resolution according to data distribution. QPA performs quantization parameter update and determines update frequency (denoted as Itv) according to the output of QEM.

4.1. Quantization Error Measurement

Based on the observation 1 and observation 3, we propose to adjust quantization parameters according to data distribution. The difference of mean before and after quantization is a good quantization error measurement, which indicates the change of data distribution and suggests the need for adjusting quantization resolution.

Intuitively, as shown in Figure. 4, the orange line and blue line represent two different data distributions. The quantization resolution is $b - a$. Using certain quantization resolution, the distribution difference can be reflected by the difference of shadow areas. Specifically, the shadow area S1 is approximately equal to S2, but S3 is much larger than S4. Therefore, for blue one, the mean after quantization $m_{\hat{x}}$ is much smaller than the original mean m_x. The difference of mean before and after quantization reflects the connection between quantization resolution and data distribution.

Mathematically, assuming that the data is under Gaussian distribution $P(x) \sim G(0, \sigma)$, and data $x \in R^p$ is quantified to $\hat{x}$. Considering the positive x, the mean between $[a, b]$ is $m_x = \frac{\int_a^b P(x)xdx}{\int_a^b P(x)dx}$, and after quantification the mean is $m_{\hat{x}} = \frac{a\int_a^c P(x)dx + b\int_c^b P(x)dx}{\int_a^b P(x)dx}$. The difference of mean before and after quantization is represented as $\frac{m_x}{m_{\hat{x}}} =$

[1]The quantification method is described in Appendix.B

Algorithm 1 Adaptive precision training. Data such as weights W_l, activations X_l and top layers' activation gradients ΔX_{l+1} of the linear layer l are quantified to fixed-point numbers with different bit-widths n and quantization resolution r. The output $Diff$ of QEM indicates the insufficiency of quantization resolution, and the output Itv of QPA determines quantization parameter update frequency.

Initial all $update\_iter = 1$
while $i < max\ iterations$ **do**
  //**Forward Propagation**
  while l in $layers$ **do**
    if $i == update\_iter_{w_l}$ **then**
      $Diff = QEM(W_l)$
      Itv,n_{w_l},r_{w_l} =$QPA(W_l, Diff)$
      $update\_iter_{w_l} = i + Itv$
    end if
    $\hat{W}_l$=Quantifiy(W_l, n_{w_l}, r_{w_l})
    if $i == update\_iter_{x_l}$ **then**
      $Diff = QEM(X_l)$
      Itv,n_{x_l},r_{x_l} =$QPA(X_l, Diff)$
      $update\_iter_{x_l} = i + Itv$
    end if
    $\hat{X}_l$=Quantifiy(X_l, n_{x_l}, r_{x_l})
    Forward:$X_{l+1} = \hat{X}_l * \hat{W}_l$//FPROP
  end while
  //**Backward Propagation**
  while l in $layers$ **do**
    if $i == update\_iter_{\Delta x_{l+1}}$ **then**
      $Diff = QEM(\Delta X_{l+1})$
      Itv,$n_{\Delta x_{l+1}}$,$r_{\Delta x_{l+1}}$ =$QPA(\Delta X_{l+1}, Diff)$
      $update\_iter_{\Delta x_{l+1}} = i + Itv$
    end if
    $\Delta\hat{X}_{l+1}$=Quantifiy($\Delta X_{l+1}, n_{\Delta x_{l+1}}, r_{\Delta x_{l+1}}$)
    Backward:$\Delta X_l = \Delta\hat{X}_{l+1} * \hat{W}_l^T$ //BPROP
    Backward: $\Delta W_l = \hat{X}_l^T * \Delta\hat{X}_{l+1}$ //WTGRAD
    //**Weight Update**
    $W_l = W_l + f(\Delta W_l)$
  end while
end while

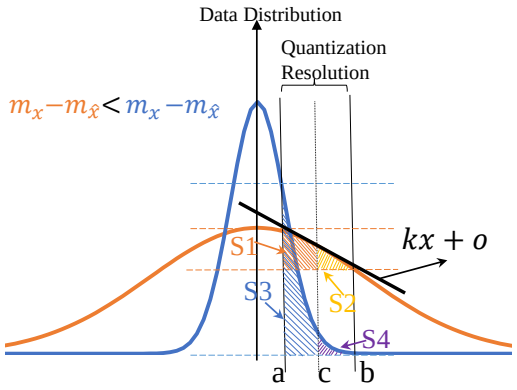

Figure 4: Data distribution and quantization resolution.

$\frac{\int_a^b P(x)xdx}{a\int_a^c P(x)dx + b\int_c^b P(x)dx}$. We use $P(x) = kx + o$ to approximate the local value between $[a, b]$ with $b < -\frac{o}{k}, k < 0$, and assign $C = \frac{1}{4}k(a+b)^2 + \frac{o(a+b)}{2}$, then we have:

$$\frac{m_x}{m_{\hat{x}}} = 1 + \frac{1/24}{\frac{C}{(b-a)^2(-k)} - 1/8} \tag{1}$$

It is demonstrated that $\frac{m_x}{m_{\hat{x}}} > 1$ and $C > 0$ (see Appendix A for details), so we have $\frac{m_x}{m_{\hat{x}}} \propto (b-a)^2 * (-k)$. When decreasing $b-a$ or increasing k, the difference of mean will be reduced. Therefore, the difference of mean serves as an explicit indicator for adjusting quantization resolution (represented by $b-a$) according to data distribution (represented by $\sigma \propto (-k)$).

Equation. 2 is used in determining quantization parameters during training.

$$\begin{aligned} Diff &= log_2(|\frac{m_x - m_{\hat{x}}}{m_x}| + 1) \\ &= log_2(|\frac{\sum_i^p |x_i| - \sum_i^p |\hat{x_i}|}{\sum_i^p |x_i|}| + 1) \end{aligned} \tag{2}$$

Larger $Diff$ indicates the distribution has higher variance σ, so it is needed to decrease quantization resolution r.

4.2. Quantification Parameter Adjustment

According to observation 2, we propose to automatically determine the quantization parameter based on the data evolution. Under the circumstance of fixed-point representation, the quantization variables include data range, quantization resolution r and bit-width n. These three variables are inter-dependent, as $Range \approx r \times 2^n$. Therefore, we use only two of them as quantization parameters (i.e., r and n). The parameter adjustment process is triggered by insufficient quantization resolution and dramatic change of data range.

For insufficient quantization resolution, we use $Diff$ as indicator. When $Diff$ exceeds certain threshold T_{data}, the quantization resolution is reduced by increasing bit-width, as $n_{new} \leftarrow n_{old} + n'$,where $n' = 8$ is the bit-width growth step. We can either set the initial $n_{old} = 8$ and recursively adjust bit-width until proper n_{new} (denoted as Mode1), or we can set the initial n_{old} as the previous iteration's proper bit-width (denoted as Mode2). The quantization resolution is adjusted according to the new bit-width n as $r = 2^{ceil(log_2(\frac{Range}{2^{n-1}-1}))}$, where $Range$ is the max absolute value of data to be quantified.

For the change of data range, we propose another indicator R for iteration i as:

$$R_i = \alpha \times Range + (1-\alpha) \times R_{i-1} \tag{3}$$

where R_i is the moving average of data $Range$ during several iterations.

The quantization parameter adjustment interval Itv is automatically determined by both $Diff$ and R. In initialization phase (one-tenth of the first epoch), Itv is set to 1. After initialization phase, the adjustment interval is $Itv = \frac{\beta}{max(I_1, I_2)} - \gamma$, as $I_1 = \delta \times Diff^2$ and $I_2 = |R_i - R_{i-1}|$. As shown in experiment, Itv increases during training. Within Itv iterations, the quantization parameters are kept the same, so there is no need to calculate $Diff$ and max absolute value of the data.

5. Experiment

We first evaluate the proposed quantization error measurement, and show the computational complexity introduced by adaptive precision. Then, we evaluate the proposed adaptive precision training on a wide variety of deep learning tasks including image classification, object detection, segmentation and machine translation in accuracy results. At last, we show the training acceleration on existing hardware.

5.1. Evaluation of Error Measurement

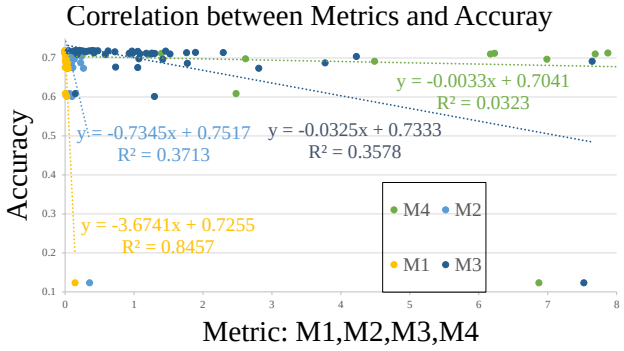

Figure 5: Correlation between MobileNet-v2 accuracy a and quantization error measurement M.

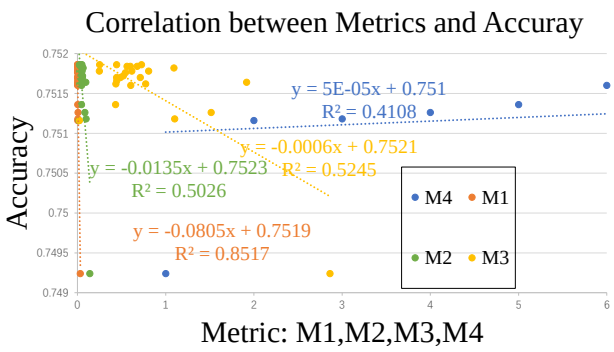

Figure 6: Correlation between ResNet50 accuracy a and quantization error measurement M.

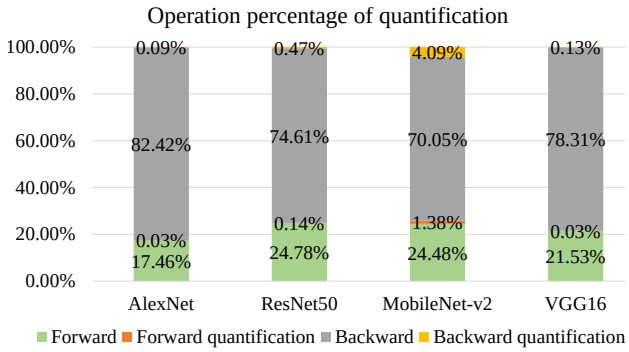

Figure 7: Operation percentage of forward and backward quantization for different models.

We use Pearson correlation coefficient in Equation. 4 to show the correlation between network accuracy a and quantization error metric M.

$$R^2 = \frac{(\sum (M - \bar{M})(a - \bar{a}))^2}{\sum (M - \bar{M})^2 \sum (a - \bar{a})^2} \tag{4}$$

The evaluated quantization error metrics including the proposed $M1 = \frac{|\sum_i |x_i| - \sum_i |\hat{x_i}||}{\sum_i |x_i|}$ and several variants: $M2 = \frac{\sum_i |x_i - \hat{x_i}|}{\sum_i |x_i|}$, $M3 = \sum_i \frac{|x_i - \hat{x_i}|}{|x_i|}$, $M4 = \sum_j P_j log(\frac{P_j}{Q_j})$. M2 is similar as in [27, 39]. M4 is the Kullback-Leibler divergence, with P_j and Q_j are the discrete probability distributions of original data and data after quantization. Specifically, we quantify each single layer of MobileNet-v2 and ResNet50 and do the forward propagation to get the corresponding network accuracy. The quantization is done with different bit-width (i.e., 6, 8), so various degrees of quantization error and the corresponding network accuracy are generated.

Figure. 5 and Figure. 6 shows the linear correlation between network accuracy and several error metrics. Our proposed quantization error measurement M1 has the highest correlation score (0.84 for MobileNet and 0.85 for ResNet50) with the network-level accuracy, which means the proposed error measurement can serve as a reasonable layer-wise accuracy indicator. MobileNet, as light-weight network, is hard to quantified as shown in Table.1, so it can exhibit the most noticeable difference between different evaluation metrics M1, M2, M3 and M4.

5.2. Computational Complexity

We evaluate the extra computations introduced by adaptive precision quantification. The extra computations including QEM, QPA and data quantification. Specifically, we calculate the operation percentage of **forward** propagation and **backward** propagation in original training, and the extra operation introduced by **forward quantification** and **backward quantification**. Figure. 7 shows the operation percentage for different networks[2]. (Details of operation quantity are shown in Appendix.B.) It is shown that for light-weight network MobileNet, the quantization consumes relatively more computations. For other networks, the extra quantization computation is within 1%.

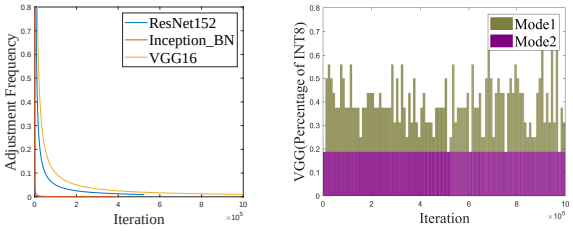

(a) (b)

Figure 8: (a)Quantification parameter adjustment frequency during training.(b)int8 percentage during training.

We evaluate the quantification parameter adjustment frequency during training. As shown in Figure. 8a, at the initial epochs, the adjustment is triggered almost every iterations, so the adjustment frequency is near 100%. As the training progress, the adjustment frequency is dramatically decreasing, and at the end of training only 0.1% iterations need to adjust the quantization parameters.

Figure. 8b shows the percentage of activation gradients quantified to int8 during training on VGG16. Mode1 allows the chance of decreasing the bit-width during training, so more percentage of layers are kept int8 (final top1 accuracy: 70.2%). In Mode2, bit-width never decreases, so at the end of training, 18.75% of layers are kept int8 (final top1 accuracy: 70.6%).

5.3. Accuracy Results

Our proposed Adaptive Precision Training approach uses identical hyper-parameters (e.g., learning rate, max training iterations) as the original float32 training settings. For all

[2]https://github.com/tensorflow/models/tree/master/research/slim

Table 1: Classification, object detection and segmentation. For all the networks, 100% weights and and 100% activations are quantified to int8.

Classification Network	**float32 Acc**	**Adaptive Acc**	**Activation Gradient** int8	int16
AlexNet	58.0	58.22	22.5%	77.5%
VGG16	71.0	70.6	31.3%	68.7%
Inception_BN	73.0	72.8	4.5%	95.5%
ResNet50	76.4	76.2	0.8%	99.2%
ResNet152	78.8	78.2	1.7%	98.3%
MobileNet v2	71.8	70.5	0.7%	99.2%
SSD Detection Network	**float32 mAP**	**Adaptive mAP**	**Activation Gradient** int8	int16
COCO_VGG	43.1	42.4	31.4%	68.6%
VOC_VGG	77.3	77.2	34.3%	65.7%
IMG_Res101	44.1	44.4	28.6%	71.4%
Segmentation Network	**float32 meanIoU**	**Adaptive meanIoU**	**Activation Gradient** int8	int16
deeplab-v1	70.1	69.9	1.0%	99.0%

tasks, we fix the bit-width for weights and activations (i.e., int8), and quantify activation gradients with adaptive bit-width. For all the tasks, we set $\alpha = 0.01$, $\beta = 0.025$, $\delta = 25$, $\gamma = 2$, $T_{topdiff} = 0.03$, and Mode2 is used in QPA.

5.3.1 Computer Vision

We train several convolution neural networks with ImageNet datasets using Tensorflow framework[3]. The networks include AlexNet [18], VGG [28], Inception_BN [29], ResNet [14] and MobileNet v2 [27][4]. We train SSD object detection networks [21][5] with VOC dataset [9], COCO dataset [20] and Imagnet Detection dataset (IMG) [25] upon two backbone networks VGG and ResNet101. We train deeplab [3][6] segmentation network on VOC dataset. For classification task, Top1 Accuracy (Acc) is used as evaluation metric. For object detection task, Mean Average Precision (mAP) is used as evaluation metric. For segmentation task, Mean Intersection over Union (meanIoU) is used as evaluation metric.

As shown in Table. 1, Adaptive Precision Training generates similar results as float32 baseline. The accuracy drop on MobileNet-v2 is consistent with the quantization results in Google's work (Acc:70.8) [16]. However, using our adaptive precision training, int8 weights can be directly deployed and no further quantified fine-tuning is needed. The proposed QPE and QPA automatically change the bit-width used for different layers. During the whole training, the percentages of different bit-width in quantization of activation gradients are shown in Table. 1[7]. For most layers of most networks, 16-bit is enough. For some layers of AlexNet and SSD, 8-bit is enough.

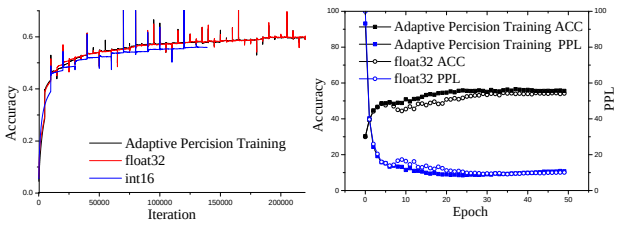

(a) Sockeye (b) Transformer

Figure 9: Machine translation.

5.3.2 Machine Translation

We train two widely used machine translation models from scratch with Adam optimizer. The first Sockeye [15] is a sequence-to-sequence RNN model implemented with MXNet [5][8], and trained on the WMT'17 news translation dataset (50k sentence pairs). The word vocabularies contain 50K entries for English and German. The second is Transformer [32][9], utilizing self-attention mechanism. This network is trained on the WMT'16 Multi30k dataset (3.9k sentence pairs). Word-level accuracy and perplexity (PPL) are used as evaluation metrics.

Training curve of Sockeye is shown in Figure. 9a. Adaptive Precision Training is compared with float32 baseline and an int16 method, which employs int16 to quantified all the layers of activation gradients without bit-width adaption. At the end of Adaptive Precision Training, 0.8% layers of activation gradients are quantified to int24, 10% layers are int8, and others are int16. As shown in Figure. 9a, the int16 method gradually results in 2% loss of accuracy, while our Adaptive Precision generates the same accuracy (62.05%) as float 32 baseline (61.97%). This comparison shows the proposed bit-width adaption is necessary to guarantee training accuracy and reduces the total bit-width in computation.

The training convergence curve of Transformer is shown in Figure. 9b. We report the accuracy and PPL on validation set. Adaptive Precision (ACC: 55.54%) is slightly better than float32 (ACC: 54.13%). On average 2.28% of iterations trigger quantization parameter adjustment.

[3]https://github.com/tensorpack/tensorpack/tree/master/examples/
[4]https://github.com/tensorflow/models/tree/master/research/slim
[5]https://github.com/weiliu89/caffe/tree/ssd
[6]https://github.com/msracver/Deformable-ConvNets

[7]This is the results of Mode2, as Mode2 generates slightly better results than Mode1, as shown in Figure. 8(b)
[8]https://github.com/awslabs/sockeye
[9]https://github.com/jadore801120/attention-is-all-you-need-pytorch

Table 2: Comparison of network quantization methods.

Methods Cited	Backward (WTGRAD/BPROP)	Adaptive Bit-width	Training from Scratch	Accuracy Degradation CNN	Accuracy Degradation RNN
[34]	float8, float16	no	yes	$<$ 1%(ResNet50)	n/a
[22]	float16	no	yes	$<$ 1%(ResNet50)	$<$ 1% (Translation)
[16]	float32	no	no	1.5% (ResNet50)	n/a
[17]	float32	no	no	$<$ 1%(ResNet18)	n/a
[6]	float32	no	yes	$<$ 1%(ResNet50)	n/a
[35]	float32	yes	no	$<$ 1%(ResNet18)	n/a
[39]	float32	yes	no	$<$ 1%(ResNet50)	n/a
[37]	float32	yes	yes	$<$ 1%(ResNet50)	n/a
[38]	int8, float32	no	yes	2.9%(AlexNet)	n/a
[36]	int8	no	yes	4%(AlexNet)	n/a
[1]	int16, float32	no	yes	$<$ 1%(ResNet50)	n/a
[7]	int16	no	yes	$<$ 1%(ResNet50)	2% (Translation)
Adaptive Precision	int8$\sim$16 (CNN) int8$\sim$24 (RNN)	yes	yes	$<$ 1%(ResNet50)	$<$ 1% (Translation)

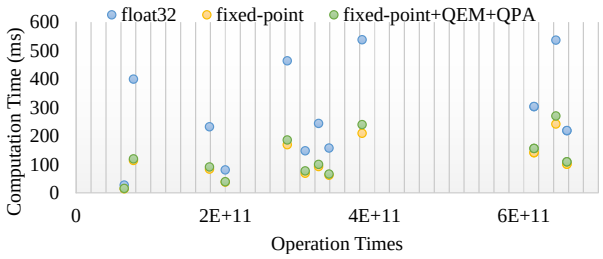

Figure 10: GPU computation time for different operation times (convolution scales).

Table 3: Layer-wise training speedup of AlexNet

	conv0	conv1	conv2	conv3	conv4
CPU Forward	2.03	3.89	6.2	4.44	4.28
CPU Backward	1.91	1.71	1.78	2.21	2.07
GPU Forward	2.82	3.63	2.97	3.01	2.72
	fc0	fc1	fc2	Overall	
CPU Forward	4.09	6.42	4.41	3.98	
CPU Backward	4.41	4.97	2.03	2.07	
GPU Forward	3.09	2.55	1.41	2.89	

5.3.3 Comparison to Others

Table. 2 shows the comparison to other quantization methods. As the accuracy of float32 baseline are different across works, we cite their relative accuracy degradation compared to their reported float32 baseline. Most works do not quantify backward-pass and are tested on convolution neural networks. Among these, [7] is the most similar method. They use int16 for both forward and backward propagation, and report results on convolution networks. Differently, we use int8 for all the forward-pass and demonstrate that for recurrent neural networks, the fixed bit-width (e.g., int16) can not meet the precision requirement for all the tasks. Therefore, it is needed to dynamically measure the bit-width requirement for different networks and tasks.

6. Training Acceleration

Intel Xeon Gold 6154 supports vector int8/int16 operations with AXV2 instruction set, and Nvidia T4 supports vector int8 operations. Table. 3 shows the speedup of our method compared with float32 in training. Specifically, we use 100 iterations' average acceleration ratio of each layer in forward-pass and backward-pass for AlexNet with 256 batch size[10]. Our approach can achieve 2.52 times speedup over float32 training on CPU, and 2.89 times speedup on GPU. Figure. 10 shows the details of running time for different type of convolution scale with different operation times. Using fixed-point the computation time is significantly shorter than float32, and the extra time introduced by QEM and QPA is relatively small.

7. Conclusion and Future Work

We observe that the data distribution reflects the precision requirement to maintain training accuracy. Therefore, we propose an adaptive precision quantization approach, which automatically determines bit-width layer-wise. Quantifying back propagation in Neural Networks can further accelerate training on hardware supporting flexible bit-width arithmetic operations. The proposed error measurement of quantization would also be extended to low-bit inference (e.g., binary or ternary), and gradient compression in the future.

[10] As T4 does not support int16, we only report the forward-pass use int8 operation. Xeon Gold 6154 can only support multiplication between equal bit-width fixed-point numbers, so in this experiment int16 $\times$ int8 is implemented as int16 $\times$ int16.

References

[1] Ron Banner, Itay Hubara, Elad Hoffer, and Daniel Soudry. Scalable methods for 8-bit training of neural networks. In *NeurIPS*, pages 5145–5153, 2018.

[2] Han Cai, Ligeng Zhu, and Song Han. Proxylessnas: Direct neural architecture search on target task and hardware. In *ICLR*, 2019.

[3] Liang-Chieh Chen, George Papandreou, Iasonas Kokkinos, Kevin Murphy, and Alan L Yuille. Deeplab: Semantic image segmentation with deep convolutional nets, atrous convolution, and fully connected crfs. *TPAMI*, 40(4):834–848, 2017.

[4] Shangyu Chen, Wenya Wang, and Sinno Jialin Pan. Deep neural network quantization via layer-wise optimization using limited training data. In *AAAI*, 2019.

[5] Tianqi Chen, Mu Li, Yutian Li, Min Lin, Naiyan Wang, Minjie Wang, Tianjun Xiao, Bing Xu, Chiyuan Zhang, and Zheng Zhang. Mxnet: A flexible and efficient machine learning library for heterogeneous distributed systems. *arXiv:1512.01274*, 2015.

[6] Jungwook Choi and Zhuo Wang. Pact: Parameterized clipping activation for quantized neural networks. *arXiv:1805.06085*, 2018.

[7] Dipankar Das, Naveen Mellempudi, Mudigere, Avancha, et al. Mixed precision training of convolutional neural networks using integer operations. In *ICLR*, 2018.

[8] Jacob Devlin, Ming-Wei Chang, Kenton Lee, and Kristina Toutanova. Bert: Pre-training of deep bidirectional transformers for language understanding. In *NAACL*, pages 4171–4186, 2019.

[9] Mark Everingham, Luc Van Gool, Christopher KI Williams, John Winn, and Andrew Zisserman. The pascal visual object classes (voc) challenge. *IJCV*, 88(2):303–338, 2010.

[10] Xavier Glorot and Yoshua Bengio. Understanding the difficulty of training deep feedforward neural networks. In *AISTATS*, pages 249–256, 2010.

[11] Suyog Gupta, Ankur Agrawal, Kailash Gopalakrishnan, and Pritish Narayanan. Deep learning with limited numerical precision. In *ICML*, pages 1737–1746, 2015.

[12] Song Han, Huizi Mao, and William J Dally. Deep compression: Compressing deep neural networks with pruning, trained quantization and huffman coding. *ICLR*, 2016.

[13] Kaiming He, Xiangyu Zhang, Shaoqing Ren, and Jian Sun. Delving deep into rectifiers: Surpassing human-level performance on imagenet classification. In *ICCV*, pages 1026–1034, 2015.

[14] Kaiming He, Xiangyu Zhang, Shaoqing Ren, and Jian Sun. Deep residual learning for image recognition. In *CVPR*, pages 770–778, 2016.

[15] Felix Hieber, Tobias Domhan, Michael Denkowski, David Vilar, Artem Sokolov, Ann Clifton, and Matt Post. Sockeye: A Toolkit for Neural Machine Translation. *arXiv:1712.05690*, Dec. 2017.

[16] Benoit Jacob, Skirmantas Kligys, Bo Chen, Menglong Zhu, Matthew Tang, Andrew Howard, Hartwig Adam, and Dmitry Kalenichenko. Quantization and training of neural networks for efficient integer-arithmetic-only inference. In *CVPR*, pages 2704–2713, 2018.

[17] Sangil Jung, Changyong Son, Seohyung Lee, Jinwoo Son, Jae-Joon Han, Youngjun Kwak, Sung Ju Hwang, and Changkyu Choi. Learning to quantize deep networks by optimizing quantization intervals with task loss. In *CVPR*, pages 4350–4359, 2019.

[18] Alex Krizhevsky, Ilya Sutskever, and Geoffrey E Hinton. Imagenet classification with deep convolutional neural networks. In *NeurIPS*, pages 1097–1105, 2012.

[19] Darryl Lin, Sachin Talathi, and Sreekanth Annapureddy. Fixed point quantization of deep convolutional networks. In *ICML*, pages 2849–2858, 2016.

[20] Tsung-Yi Lin, Michael Maire, Serge Belongie, James Hays, Pietro Perona, Deva Ramanan, Piotr Dollár, and C Lawrence Zitnick. Microsoft coco: Common objects in context. In *ECCV*, pages 740–755. Springer, 2014.

[21] Wei Liu, Dragomir Anguelov, Dumitru Erhan, Christian Szegedy, Scott Reed, Cheng-Yang Fu, and Alexander C Berg. Ssd: Single shot multibox detector. In *ICCV*, pages 21–37. Springer, 2016.

[22] Sharan Narang, Gregory Diamos, Elsen, et al. Mixed precision training. *ICLR*, 2018.

[23] NVIDIA. Nvidia tesla v100 gpu architecture. 2017.

[24] Andres Rodriguez, Eden Segal, et al. Lower numerical precision deep learning inference and training. *Intel White Paper*, 2018.

[25] Olga Russakovsky, Jia Deng, et al. Imagenet large scale visual recognition challenge. *IJCV*, 115(3):211–252, 2015.

[26] Charbel Sakr and Naresh Shanbhag. Per-tensor fixed-point quantization of the back-propagation algorithm. In *ICLR*, 2019.

[27] Tao Sheng, Chen Feng, Shaojie Zhuo, Xiaopeng Zhang, Liang Shen, and Mickey Aleksic. A quantization-friendly separable convolution for mobilenets. In *EMC2*, pages 14–18. IEEE, 2018.

[28] Karen Simonyan and Andrew Zisserman. Very deep convolutional networks for large-scale image recognition. *arXiv:1409.1556*, 2014.

[29] Christian Szegedy, Vincent Vanhoucke, Sergey Ioffe, Jon Shlens, and Zbigniew Wojna. Rethinking the inception architecture for computer vision. In *CVPR*, pages 2818–2826, 2016.

[30] Stefan Uhlich, Lukas Mauch, Kazuki Yoshiyama, Fabien Cardinaux, Javier Alonso García, Stephen Tiedemann, Thomas Kemp, and Akira Nakamura. Differentiable quantization of deep neural networks. *arXiv preprint arXiv:1905.11452*, 2019.

[31] Yaman Umuroglu, Lahiru Rasnayake, and Magnus Själander. Bismo: A scalable bit-serial matrix multiplication overlay for reconfigurable computing. In *FPL*, pages 307–3077. IEEE, 2018.

[32] Ashish Vaswani, Noam Shazeer, Niki Parmar, Jakob Uszkoreit, Llion Jones, Aidan N Gomez, Łukasz Kaiser, and Illia Polosukhin. Attention is all you need. In *NeurIPS*, pages 5998–6008, 2017.

[33] Kuan Wang, Zhijian Liu, Yujun Lin, Ji Lin, and Song Han. Haq: Hardware-aware automated quantization with mixed precision. In *CVPR*, pages 8612–8620, 2019.

[34] Naigang Wang, Jungwook Choi, Daniel Brand, Chia-Yu Chen, and Kailash Gopalakrishnan. Training deep neural networks with 8-bit floating point numbers. In *NeurIPS*, pages 7675–7684, 2018.

[35] Bichen Wu, Yanghan Wang, Peizhao Zhang, Yuandong Tian, Peter Vajda, and Kurt Keutzer. Mixed precision quantization of convnets via differentiable neural architecture search. *arXiv:1812.00090*, 2018.

[36] Shuang Wu, Guoqi Li, Feng Chen, and Luping Shi. Training and inference with integers in deep neural networks. In *ICLR*, 2018.

[37] Jiwei Yang, Xu Shen, Jun Xing, Xinmei Tian, Houqiang Li, Bing Deng, Jianqiang Huang, and Xiansheng Hua. Quantization networks. In *CVPR*, June 2019.

[38] Shuchang Zhou, Yuxin Wu, Zekun Ni, Xinyu Zhou, He Wen, and Yuheng Zou. Dorefa-net: Training low bitwidth convolutional neural networks with low bitwidth gradients. *arXiv:1606.06160*, 2016.

[39] Yiren Zhou, Seyed-Mohsen Moosavi-Dezfooli, Ngai-Man Cheung, and Pascal Frossard. Adaptive quantization for deep neural network. In *AAAI*, 2018.

8. Appendix A

The difference of mean value before and after quantization is $\frac{m_d}{m_{\hat{d}}} = \frac{\int_a^b P(x)xdx}{a\int_a^b P(x)dx + b\int_a^b P(x)dx}$. We use $P(x) = kx + o$ to approximate the local value between $[a, b]$ with $b < -\frac{o}{k}, k < 0$, and assign $C = \frac{1}{4}k(a+b)^2 + \frac{o(a+b)}{2}$, then we have:

$$\begin{aligned}\int_a^b P(x)xdx &= \int_a^b (kx^2 + ox)dx \\ &= \frac{1}{3}kx^3 + \frac{1}{2}kx^2\Big|_a^b \\ &= (\frac{1}{3}k(a^2+b^2+ab) + \frac{o}{2}(a+b))(b-a)\end{aligned} \tag{5}$$

$$\begin{aligned}a\int_a^c P(x)dx + b\int_c^b P(x)dx &= a\int_a^c (kx+o)dx + b\int_c^b (kx+o)dx \\ &= a\,(\frac{1}{2}kx^2 + ox)\Big|_a^c + b\,(\frac{1}{2}kx^2 + ox)\Big|_c^b \\ &= (\frac{1}{8}k(3a^2+3b^2+2ab) + \frac{o}{2}(a+b))(b-a)\end{aligned} \tag{6}$$

$$\frac{m_d}{m_{\hat{d}}} = \frac{\frac{1}{3}k(a^2+b^2+ab) + \frac{o}{2}(a+b)}{\frac{1}{8}k(3a^2+3b^2+2ab) + \frac{o}{2}(a+b)} \tag{7}$$

$$\frac{1}{3}k(a^2+b^2+ab) - \frac{1}{8}k(3a^2+3b^2+2ab) = -\frac{1}{24}(a+b)^2k > 0 \tag{8}$$

Considering Equation. 8 in Equation. 7 , we have $\frac{m_d}{m_{\hat{d}}} > 1$. Denote $A = a + b$ and $B = b - a$, then Equation. 7 becomes:

$$\frac{m_d}{m_{\hat{d}}} = \frac{\frac{1}{4}kA^2 + \frac{1}{2}oA + \frac{1}{12}kB^2}{\frac{1}{4}kA^2 + \frac{1}{2}oA + \frac{1}{8}kB^2} \tag{9}$$

As $b < -\frac{o}{k}$, so $\frac{k}{o} > -\frac{1}{b}$

$$\begin{aligned}C &= \frac{1}{4}kA^2 + \frac{1}{2}oA \\ C &= \frac{1}{4}Ao(\frac{k}{o}A + 2) > \frac{1}{4}A\frac{b-a}{b} > 0\end{aligned} \tag{10}$$

Therefore,

$$\begin{aligned}\frac{m_d}{m_{\hat{d}}} &= \frac{C + \frac{1}{12}kB^2}{C + \frac{1}{8}kB^2} \\ &= 1 - \frac{1/24}{\frac{C}{B^2k} + 1/8} \\ &= 1 + \frac{1/24}{\frac{C}{(b-a)^2(-k)} - 1/8}\end{aligned} \tag{11}$$

Appendix B. Quantification Method

A fixed-point number consists of a sign bit, $(n-1)$-bit integer, and a global quantization resolution r relating to fixed-point position s. Before quantization, the maximum absolute data is Z. The representation data range, bit-width and quantization resolution are inter-dependent, as $Range \approx r \times 2^n$. The quantization resolution is calculated as in Table. 4 column 2. Suppose F_x is the floating point representation of x and I_x is the fixed-point representation of x, and $\hat{F_x}$ is the approximation of F_x, as $\hat{F_{x_1}} = I_{x_1} \times r_1$, $\hat{F_{x_2}} = I_{x_2} \times r_2$, the multiplication between numbers becomes:

$$F_{x_1} \times F_{x_2} \approx \hat{F_{x_1}} \times \hat{F_{x_2}} = r_1 \times r_2 \times I_{x_1} \times I_{x_2} \tag{12}$$

Table 4: Quantization schemes (scheme 1 most efficient, scheme 3 most accurate)

Quantization Function	Quantization Scale	Fixed-point Range
$I_x = round(\frac{F_x}{r})$	$r = 2^s = 2^{ceil(log_2(\frac{Z}{2^{n-1}-1}))}$	$[-r(2^{n-1}), r(2^{n-1}-1)]$

Appendix C. Observations on Other Network

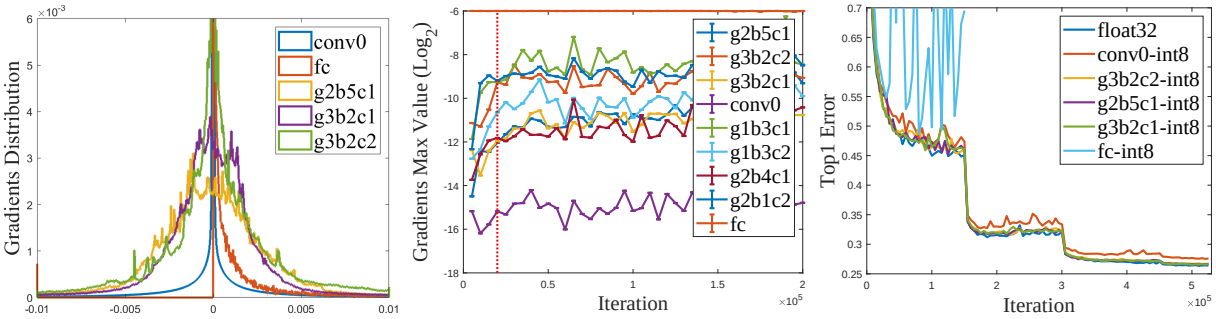

(a) Activation gradient distribution. (b) Activation gradient evolution. (c) Training curve of AlexNet.

Figure 11: Observations on ResNet34.

As shown in Figure. 11, for ResNet34 int8 is enough to quantify the activation gradient of g3b2c2, g2b5c1 and g3b2c1, however, int8 for fc and conv0 either not converges or introduces accuracy drop, conv0 and fc have large variance. These observations are consistent with the observation on AlexNet. In conclusion, data with large variance requires large bit-width, thus the quantization parameters should be dynamically determined by the data distribution.

Appendix D. Operation Quantity

Table 5: Operations for different networks

	AlexNet	ResNet50	MobileNet-v2	VGG16
Forward	3.78E+11	1.78E+12	1.54E+11	7.93E+12
Forward Quantification	6.95E+08	1.01E+10	8.68E+09	1.24E+10
Backward	1.78E+12	5.37E+12	4.41E+11	2.88E+13
Backward Quantification	1.90E+09	3.39E+10	2.57E+10	4.70E+10

Appendix E. Speedup over int16

There is 1.3 times speedup over int16 on CPU for AlexNet (1.13 times speedup for backward and 1.7 times speedup for forward). The int16 x int8 in our method is implemented as int16 x int16 on Xeon Gold 6154. With flexible arithmetic operations like int16 x int8 on future hardware, higher training speedup is promising.